6-1-1980

Design and production of a comprehensive graininess scale for use in electrophotography

Susan B. Mueller

School of Printing
Rochester Institute of Technology
Rochester, New York

CERTIFICATE OF APPROVAL

MASTER'S THESIS

This is to certify that the Master's Thesis of

Susan Barbara Mueller

with a major in Printing Technology has been approved by the Thesis Committee as satisfactory for the thesis requirement for the Master of Science degree at the convocation of June, 1980.

Thesis Committee:

_____
Thesis Advisor

_____
Thesis Advisor

_____
Graduate Advisor

_____
Director or Designate

DESIGN AND PRODUCTION OF A COMPREHENSIVE GRAININESS SCALE FOR USE IN ELECTROPHOTOGRAPHY

by

Susan B. Mueller

A thesis submitted in partial fulfillment of the requirements for the degree of Master of Science in the School of Printing in the College of Graphic Arts and Photography of the Rochester Institute of Technology

June, 1980

Thesis advisors: Professor John Carson

Dr. Rodney Shaw

ACKNOWLEDGMENTS

I would like to extend my sincere appreciation to my thesis advisors, Professor John Carson, Dr. Rodney Shaw, and Dr. Julius Silver, for their time and assistance in this study.

I would also like to thank Xerox corporation for its support, especially my friends Roger Dooley, Robert Davis, and Barbara Bellucci.

TABLE OF CONTENTS

TABLE OF CONTENTS cont.

LIST OF FIGURES

Figure

LIST OF FIGURES cont.

Figure

ABSTRACT

Methods were investigated and modeled to produce a graininess by density sample matrix. The graininess values were based on a model derived for certain imaging processes that has a high correlation to the subjective impression of graininess for nominally uniform image areas. After modeling several processes, a photographic technique was chosen and a matrix manufactured.

Abstract approved: J F Cawe thesis advisor

Associate Prof. title

Rodney Bra thesis advisor

Ph. D. title

5/16/80 date

CHAPTER I

INTRODUCTION

The visual sensation of random non-uniformity in an image which is nominally uniform has acquired the name graininess. Objective correlations to graininess may be made via some measurement of reflection density or reflectance fluctuations about the mean level. These fluctuations are frequently characterized by rms granularity, although more complete characterization is possible by measurement of the Weiner Spectrum, (WS), as a function of spatial frequency. (See Appendix A.)

Attempts to analyze the noise characteristics of recorded photographic images have been documented in the literature[1]. Photographic images are composed of particles that are largely spatially independent, and further, image density is a function of the number of developed silver halide particles[2]. Noise in other imaging processes exhibiting the same characteristics, such as electrophotography[3], may be analyzed by the same methods as photographic images.

Basic work to model the noise in silver photographic images was done by Selwyn and Siedentopf in the 1930's[4]. Both derived objective relationships that could be used to

characterize the physical noise of an image.

The Selwyn granularity coefficient, S, is defined:

$$S = \sigma_A\sqrt{2A} \qquad (1)$$

where σ_A = root mean-square fluctuation in density of a sample and A = area of the scanning aperture. The Siedentopf relationship for image noise, G:

$$G = \log_{10} e\bar{a}_D D \qquad (2)$$

where $\bar{a}_D$ is the mean projection area of a grain and D is average image density. These original noise measurements and those that have subsequently evolved are often used to help in the characterization of the graininess of an image, augmented by simple assumptions concerning visual response.

Recently a graininess model has been derived by Dooley and Shaw[5] for imaging processes producing images governed by the relationships mentioned above for photographic images:

$$GS = e^{-1.8D}\int_0^\infty \sqrt{WS(u)}\ VTF(u)du \qquad (3)$$

The model makes use of the visual transfer function[6] for

the human eye:

$$VTF(u) = \begin{cases} (5.05e^{-.843u})(1-e^{-0.61u}) & u > .8 \\ 1 & u \leq .8 \end{cases} \quad (4)$$

(See Appendix B.) The abbreviation WS(u) refers to the Weiner (noise-power) Spectrum of the density fluctuations at a particular spatial frequency, u. The term $e^{-1.8D}$ takes into account the sensitivity of the human response to fluctuations in density as a function of the mean reflection density level, D. Graininess values predicted with this model had a 0.97 correlation coefficient with values obtained using human observers. On the Dooley and Shaw scale a graininess of 0 is equal to a smooth homogeneous surface. White bond paper typically has a graininess value of 1 to 3 on this scale. A graininess of 30 corresponds to a fairly high level of noise in an electrophotographic image. (See Figure 9.) At background densities of 0 to 0.3 a Just Noticable Difference (JND) in graininess is on the order of 0.7 graininess units. At a density of 0.4, a JND is approximately 1.5 graininess units, and at high densities a JND is approximately 2.5 graininess units.

This investigation concerns the design, development and production of a matrix of samples that meet particular

graininess and reflection density requirements, to serve as a visual measuring device to estimate the graininess of solid area positive images.

FOOTNOTES FOR CHAPTER I

1. a.Rodney Shaw,(Ed.), Selected Readings in Image Evaluation, (SPSE Publication,1976).

   b.A. Marriage and E. Pitts, "Relation between Granularity and Auto-correlation",J. Opt. Soc. of Amer., 46, 1019-1027.

2. a.Rodney Shaw, "Equivalent Quantum Efficiency of Photographic Emulsions", J. Phot. Sci., 13, 1965, 308-317.

   b.R.H. Ericson and J.C. Marchant, "RMS Granularity of Monodisperse Photographic Emulsions", Phot. Sci. Eng., 16, 1972, 253-257.

3. a.Rodney Shaw, "Comparative Signal-to-Noise Ratio Analysis of Particle Development in Electrophotography and Silver Halide Photography", J. Appl. Phot. Eng., 1, 1975, 1-4.

   b.J. VanEngeland, W. Verlinden and J. Marien, "Granularity of Electrophotographic Images", J. Phot. Sci., 25, 1977, 154-158.

   c.R.N. Goren, and J.F. Szczepanik, "Image Noise of Magnetic Brush Development", Photo. Sci. Eng., 22, 1978, 235-239.

4. J.C. Dainty and Rodney Shaw, Image Science (Academic Press, 1974), 58-60, 98.

5. Roger P. Dooley and Rodney Shaw, "Noise Perception in Electrophotography", J. Appl. Phot. Eng., 4, 1979, 190-196.

6. ibid.

CHAPTER II

THEORETICAL

1.0 Matrix requirements

In order to assemble a graininess by density matrix the sample parameters had to be established prior to determination of sample production techniques. The sample matrix was designed to encompass both the density range of images produced by standard electrophotographic copiers, typically 0 to 1.4 density units, and the practical graininess range for electrophotographic copiers, typically 2 to 30 graininess units on the graininess scale.

2.0 Method of manufacture

A review of the literature shows that much of the theoretical work to understand the fundamentals of image noise has involved mathematical modeling, and little work has been done on noise simulation. Although references 10-12 describe simulated noise samples in experimental situations, the actual methods of production are not completely explained, or are not practically relevant to

this project. Methods used to produce noise samples include magnification of photographic grain, imaging laser speckle, computer-generated random dot samples, and imaging ground glass.

Each method was considered in terms of equipment and facilities available and the time involved in production. Based on these considerations it was decided to attempt to use computer-generated noise samples. A computer program generated random number pairs to specify the x and y coordinates of a specified number of points within an area of 3.18 x 3.18 cm^2. (Details of the computer program are given in Appendix C.) The x and y values generated were read into an Information Systems International FR80 computer controlled CRT graphics camera. The x and y coordinates located the electron beam position on the CRT. Optical reduction of the CRT face to a 35mm format made it possible to record the random noise sample photographically. The image parameters available for user manipulation via the computer program included the location of points, number of points drawn, point brightness, and the number of hits each point receives. A hit refers to drawing a point on the CRT and blanking the screen. This procedure is repeated for each hit requested. The image parameters available for manipulation by the FR80 operator included image intensity, focus and quality of film processing.

The point brightness, the number of hits, and the image intensity all control the exposure at each point.

The processed film samples were contact printed to glass plates, and the glass plates contact printed to photographic paper to produce the reflection samples. The glass plates were stored for future reproduction of the matrix.

3.0 Preliminary experiments

Preliminary tests indicated that the maximum number of points that could be written with the program was not large enough to produce the graininess range of 0 - 30. The maximum number of points that could be written was 1.1×10^6, which was calculated to correspond to a graininess of approximately 16. Therefore it was necessary to vary the number of hits as well as the number of points to produce the required graininess range. A preliminary experiment was developed to generate a range of samples, varying in both the number of hits and the number of points. The results of this experiment were to be used to predict the correct combinations of number of hits and number of points required to produce each graininess by density sample in the matrix.

Two significant problems arose. The first was due to inconsistent processing of the film resulting in density variations between images as well as within one image. Image quality standards required for this project were much higher than the standards for general use of the FR80 equipment, so the problem was most easily remedied by hand-processing the film. The second problem then emerged. Frequently the film was fogged. It was impossible to pinpoint the source of the fog because its location on the film varied from occasion to occasion. The project could not be completed in a reasonable time if the images that were fogged had to be continually monitored and regenerated. It was decided to produce the matrix using one film sample of the smallest dot size that had a uniform image density across the entire sample, i.e. no visible patterns or mottle on the sample. The sample negative consisted of one million points, three hits for each point. This sample negative was enlarged onto high contrast plates at different magnifications. Each plate was exposed and developed to approximately the same overall density. Each plate was then contact printed to photographic paper at different exposure levels to produce the different densities.

4.0 Mathematical prediction of results

Predictability and repeatability for the graininess noise samples was of utmost importance. To manufacture the matrix it was necessary to produce values of graininess and density within limited tolerances. The graininess tolerance for the entire matrix corresponds to the JND value at low densities, ±0.7 graininess unit. The density tolerance corresponds to the equivalent of ±1/4 step in the Munsell value scale, V, where

$$V = 2.468[(R)(100)]^{1/3} - 1.636 \qquad (5)$$

R refers to sample reflectance.

By inspection of the nature of the graininess algorithm it is seen that samples differing in both Weiner Spectrum and density may appear equally grainy to an observer. This effect is the consequence of the non-linear relationship between density and brightness such that density fluctuations are much less visible at high densities than at low ones. The shape of the graininess by density function may be predicted by multiplying the sensitivity term $e^{-1.8D}$ and a plot of WS(0), as in Figure 1. As density increases there is a linear increase in WS(0). The few particles at low densities result in little power in the Weiner Spectrum at

these densities. Hence values of the graininess by density function will be low. At high densities, however, decrease in visual sensitivity to density fluctuations forces the graininess by density curve to decline. Hence the graininess by density curve peaks at middle densities.

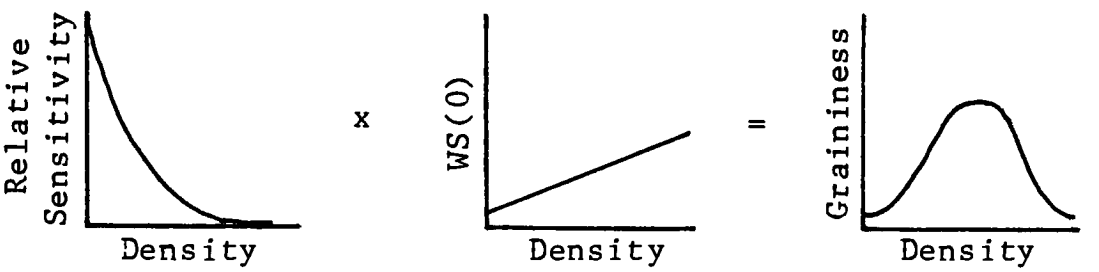

Prediction of Graininess by Density Function

Figure 1

The mathematical prediction of graininess at a specific mean density level requires calculations based on equation (3). The VTF(u) was defined in equation (4). If the WS(u) is constant over the frequency range of interest, examination of equation (3) and Figure 2,

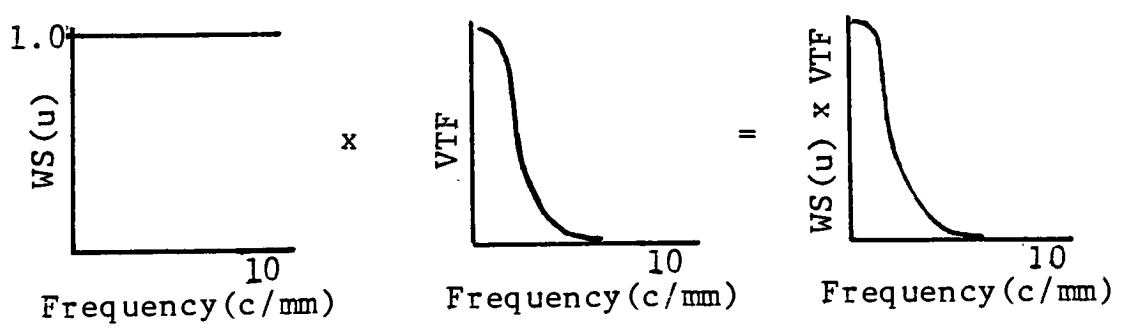

Cascading WS(u) and VTF

Figure 2

reveals that the VTF will be the limiting function in graininess-frequency response. The VTF is effectively zero at 8 c/mm. The reflection density value, D, for the term, $e^{-1.8D}$, corresponds to the chosen mean reflection density of the sample. The remaining term to be determined was WS(u). A first approximation was developed.

A first approximation of WS(u) is WS(0), and for opaque particles of area, a, the Nutting equation, (6) may be used to arrive at an estimate of WS(0). As indicated in Figure 3, suppose an area A includes N opaque particles of area a:

$$\bar{D} = \log_{10} e\left(\frac{Na}{A}\right) \qquad (6)$$

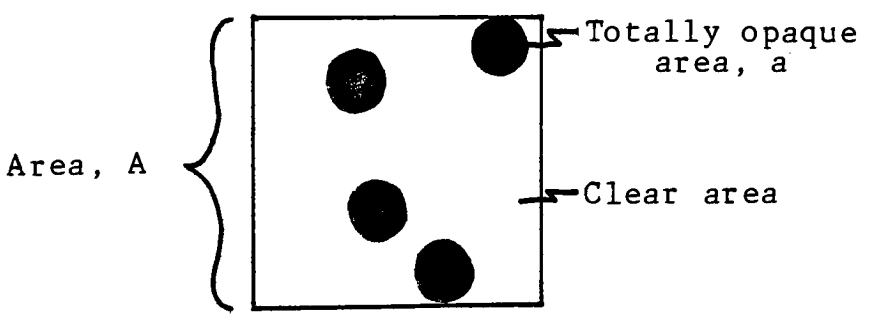

Area A of Totally Opaque Particles

Figure 3

If the particles are spatially-distributed according to Poisson statistics, the variance of N will be equal to the mean value of N, as seen on the following page.

$$\sigma_N^2 = \bar{N} \qquad (7)$$

Combination of equations (6) and (7) then leads to an abbreviated form of Siedentopf's equation:

$$\sigma^2(\bar{D}) = \left(\frac{.434a}{A}\right)\bar{D} \qquad (8)$$

This equation relates the image density fluctuations, (noise), to the fluctuations in numbers and geometry of the image particles.[1] For the special case of particles all the same size the Siedentopf equation reduces to:

$$A\sigma^2(\bar{D}) = .434a\bar{D} \qquad (9)$$

As a first approximation the fluctuations $A\sigma^2(\bar{D}) = WS(0)$, therefore:

$$WS(0) = .434a\bar{D} \qquad (10)$$

If the particles are small, WS(0) will be approximately constant for spatial frequencies whose period is much greater than the dimensions of a particle. This is illustrated in Figure 4.

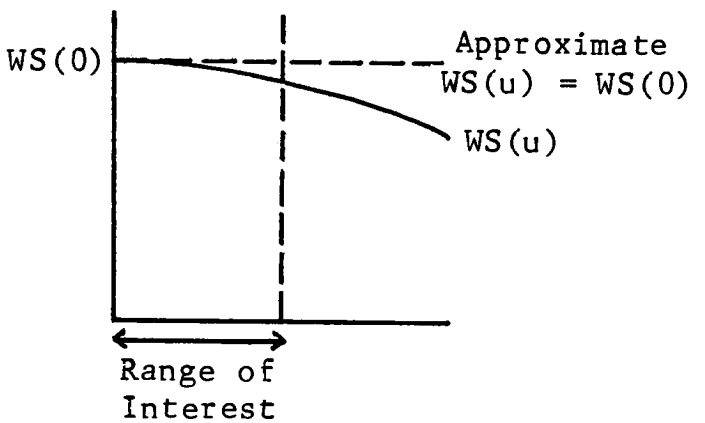

Weiner Spectrum of Small Particles

Figure 4

To a first approximation, over the frequencies of interest (0 - 8 c/mm) the WS(u) of the photographic film, plate and paper combination may be considered to be approximately constant. Both the film and plate emulsions are fine grain, high resolution emulsions which would be expected to have a Weiner Spectrum that is constant over a greater frequency range than films such as Tri-X or Pan-X. The latter films contain particle sizes larger than those of the film and plate emulsions used in this experiment. The larger particle sizes will result in a lower frequency cut-off of the Weiner Spectrum. The WS(u)

of both of the latter films are published for specific conditions of exposure and development. Both are constant below 8 c/mm^2 as is shown in Figure 5.

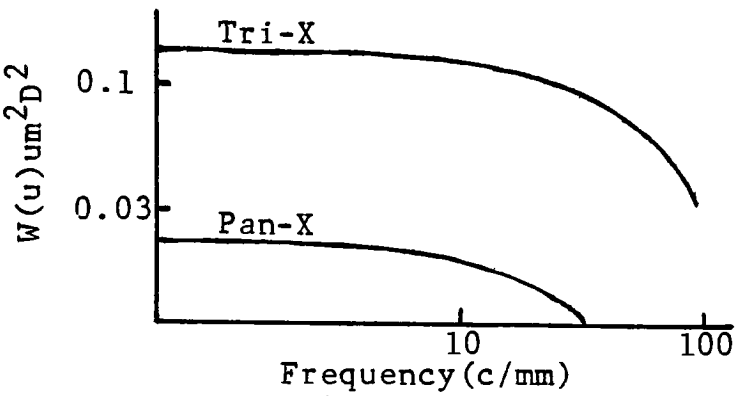

Weiner Spectrum for Tri-X and Pan-X

Figure 5

Data is available on the paper MTF at one mean reflection density level[3]. Figure 6 illustrates the paper MTF as a constantly decreasing function that cuts off at approximately 40 c/mm.

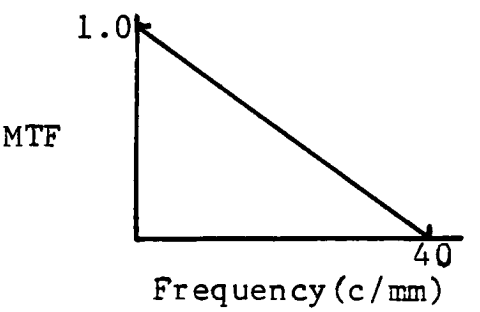

MTF of Chronapaque Paper

Figure 6

The graininess equation, (3), may be rewritten with WS(u) as a constant, WS(0):

$$GS = e^{-1.8D\sqrt{WS(0)}} \int_0^\infty VTF(u)du \qquad (11)$$

The value of the integral is approximately equal to 2.7 for the frequency range of interest, 0 to 10 c/mm, and the graininess equation now becomes:

$$GS = 2.7e^{-1.8D\sqrt{WS(0)}} \qquad (12)$$

In dealing with a photographic paper sample that is produced via a film positive contacted to glass plate and then to paper, the particles are not necessarily opaque. They will be characterized by a reflectance, r. Therefore a new model is needed for WS(0) to take into account the particle reflectance. The relationship between density and reflectance has been investigated by Bayer[4], Berwat[5], and others. Figure 7 on the following page displays a large area, A, with N particles of area, a, each having a reflectance, r_a. Equation (13) on the following page describes the reflectance, R_A, of the large area, A, as the ratio of the reflectance of clear area to the reflectance of the total area.

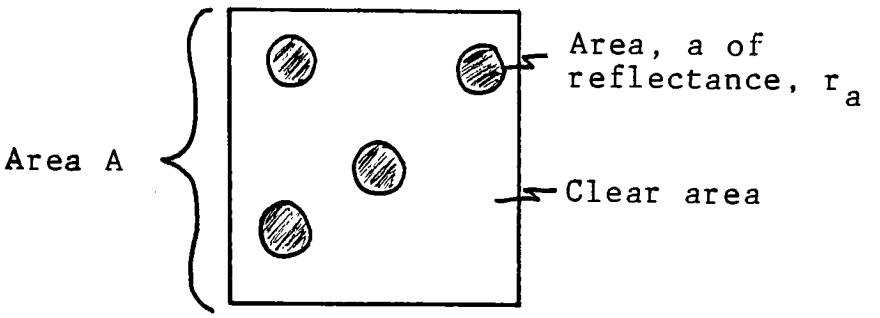

Area A of Particles with Reflectance, r_a

Figure 7

$$R_A = \frac{Ai_o - Nai_a}{Ai_o} \qquad (13)$$

Where i_o is the total incident flux/area, and i_a is the flux/area absorbed by each area a. Rearranging the previous equation:

$$R_A = \frac{1 - \frac{Nai_a}{Ai_o}}{1} \qquad (14)$$

and realizing $i_a + i_r = i_o$ where i_r is equal to the flux/area reflected by small area a, and $r_a = i_r/i_o$:

$$R_A = \frac{1 - \frac{Na\,(i_o - i_r)}{Ai_o}}{1} = \frac{1 - \frac{Na}{A}\,(1-r_a)}{1} \qquad (15)$$

Set $x = \frac{Na}{A}(1-r)$:

$$\bar{D} = -\log_{10} R_A = -.434 \log_e R_A \qquad (16)$$

$$\bar{D} = -.434 \log_e \left(\frac{1-x}{1} \right) \qquad (17)$$

For small values of x, $\log_e(1+x) = x$, therefore:

$$\bar{D} = .434x = .434 \frac{Na(1-r_a)}{A} \qquad (18)$$

Equation 16 expresses the average reflection density of the light reflected from a large area, A, with N particles of area a, and reflectance r_a. Poisson statistics again determine the variance in reflection density of the area A:

$$\sigma^2(\bar{D}) = \left(\frac{.434a(1-r_a)}{A}\right)\bar{D} \qquad (19)$$

Using the Siedentopf relationship to relate image density fluctuations to the fluctuations in numbers and geometry of the image particles:

$$A\sigma^2(\bar{D}) = .434a(1-r_a)\bar{D} = WS(0) \qquad (20)$$

The constant .434 may be replaced by a constant k, which may be considered a system variable peculiar to the particular experimental procedures and measurements of the reflection samples. There are now three equations to use to model the data:

$$\bar{D} = kna(1-r_a) \qquad \text{where } n = \frac{N}{A} \qquad (21)$$

$$WS(0) = ka(1-r_a)\bar{D} \qquad (22)$$

$$GS = 2.7e^{-1.8D}\ WS(0) \qquad (23)$$

It is now possible with these equations to compute curves of graininess vs. density for selected values of r, n, and a. These curves are used as a guide to produce the samples for the matrix. The curves are then compared with the actual experimental results to determine the accuracy of this model.

This model assumes the dots are round, randomly placed and do not overlap. Dot overlap may be a significant factor in the fit of the model to the experimental data. Bayer[6] found a significant difference in values between a model that takes dot overlap into account and a model that does not. The values for the WS(0) are higher for the dot overlap model.

FOOTNOTES FOR CHAPTER II

1. J.C. Dainty and Rodney Shaw, Image Science (Academic Press, 1974), 58-60, 97-99.

2. ibid. 309.

3. Personal correspondence with James J. Jakubowski, Xerox employee, Webster, N.Y.

4. B.E. Bayer, "Relation Between Granularity and Density for a Random-Dot Model", J. Opt. Soc. of Amer., 54, 1964, 1485-1490.

5. L. Berwart, "Weiner Spectrum of Experimental Emulsions with Cubic Homogeneous Grains, Comparison of the Spectra with the Wiener Spectra of Commercial Emulsions", J. Phot. Sci., 17, 1969, 41-47.

6. op. cit. B.E. Bayer

CHAPTER III

OBJECTIVE

The production of a graininess by density matrix has been discussed from a theoretical standpoint. The objective of the experimental work was to produce samples of specific graininess and reflection density. Computing facilities and photographic materials and methods were used to produce the samples.

CHAPTER IV

METHODOLOGY

1.0 Sample production

Sample production for the graininess by density matrix was accomplished photographically. As described in the theoretical section the original film positive was produced via a computer program that generates random number pairs to specify the x and y coordinates of a specified number of points within an area of 3.15 x 3.15 cm^2. The sample used consisted of one million points, each point receiving three hits at a brightness level of 45. These specifications produced an image of uniform density across the entire sample. The x and y values generated, number of hits per point, and brightness level requested were read into the FR80 computer-controlled graphics camera. The x and y coordinates located the electron beam position on the CRT. Optical reduction of the CRT face to a 35 mm format facilitated photographically recording the random noise sample within a 3.15 x 3.15 cm^2 format. The image was recorded on Kodak Recordak AHU microfilm.

The exposed film was then processed in a Nikor tank to a negative image. All processing data is presented in Appendix D. The positive transparency was enlarged or reduced onto Kodak PFO ortho plates. Magnifications used were: .8X, 1X, 1.25X, 1.5X, 1.75X, 2X, and 3X. A standard Omega enlarger with Schneider-Componar 80 mm and 135 mm lenses was used. The enlarger configuration of image, s', and object, s, distances were closely approximated with the imaging equations:

$$s = f(1+1/m) \qquad (24)$$

$$s' = f(m+1) \qquad (25)$$

where f is the focal length in mm of the lens, and m is the magnification. Final adjustment of the enlarger was made by measuring the size of the image to determine that the magnification was correct. A grain focuser was used to focus at the image plane. Typical conditions for 2X magnification were: 135 mm lens, f/8, .4 N.D., 1.1 second exposure. Each plate was exposed to produce an optical transmission density of approximately 0.75 after processing. It was difficult to measure the density accurately on a transmission densitometer with 2.0 mm aperture because the magnification was different on each plate. A .8X and 1.5X plate were exposed and processed to

a much higher density to predict and observe the measured effect. Two .8X plates were defocused, and exposed and processed to the standard density to predict and observe the measured effects.

Each plate was contact printed to DuPont Chronapaque Print Film to produce a series of reflection samples from each plate at different densities. A contact printing frame illuminated by a tungsten point source was used. The lowest vacuum pressure was used to maintain a constant, repeatable pressure and avoid Newton's rings. The exposures were all made at the same location in the frame and exposed with a variable time integrator. The exposure was modulated at the point source with neutral density filters to produce the series of reflection samples. Each exposed sample was then processed per the solutions and instructions for Chronapaque listed in Appendix D.

2.0 Sample measurement

A one inch square sample area was marked on each image and this area was read on a reflection microdensitometer. The microdensitometer had a standard ANSI configuration for measuring reflection density. Effective slit dimensions of 1000 x 25.4 um were used in the scanning.

N = 50 digital readings were taken at a constant sampling interval of x = 25.4 um. This results in a WS resolution of (1/N x) of approximately 0.8 c/mm up to a Nyquist frequency (1/2 x) of 20 c/mm. The Nyquist frequency refers to the maximum frequency to which the calculation may be carried. M = 40 data sets then reduced the standard error in the spectrum estimate to 1/40 or approximately 16%. The graininess value described by equation (3) was calculated via computer. The 2000 total values (50 readings x 40 data sets) were read into a standard computer program that automatically calculated the Weiner Spectrum values and square roots. These values were multiplied by the VTF, integrated, and then multiplied by the factor $e^{-1.8D}$ to determine the graininess value. The program output, Figures 13 and 14, consisted of a plot of the WS, and the calculated density and graininess of the sample.

3.0 Mathematical prediction

Prediction of the shape of the graininess by density function was made prior to any reflection sample production and measurement. This was done for the 1X, 2X, and 3X cases. The predicted values are plotted in Figure 8. The k term was ignored and equations (22) and (23)

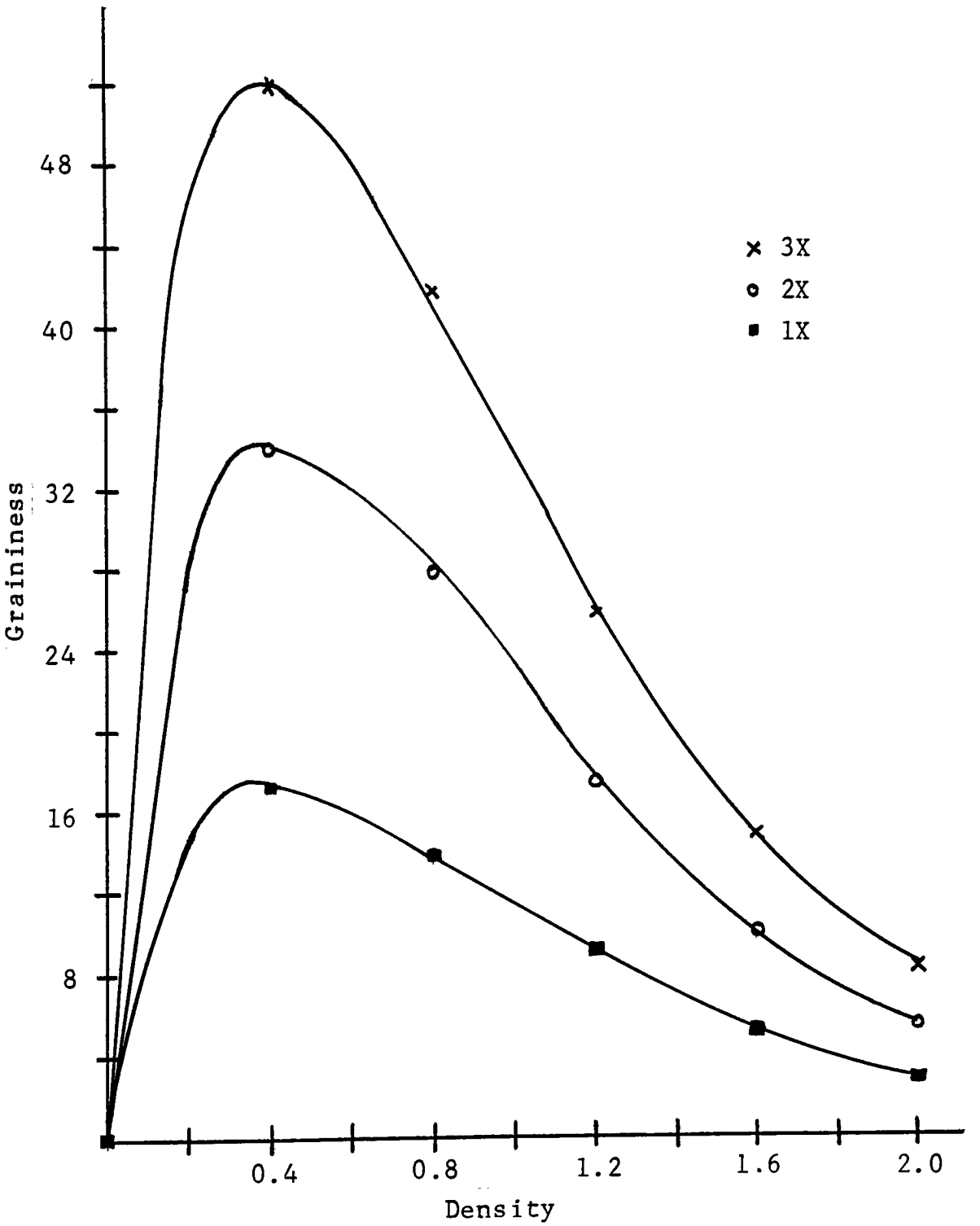

Predicted Graininess Values Ignoring k Value

Figure 8

were used with selected densities from 0 to 2.0. The reflectance r_a was approximated by the equation:

$$r = 10^{-D} \tag{26}$$

D refers to the measured density of substrate and image. $\bar{D}$ refers to the image density minus the substrate density. A Chronapaque base density of 0.15 was measured on the reflection microdensitometer. The reflection microdensitometer is zeroed relative to Barium Sulfate. The area, a, of a particle was calculated using the average diameter of the dots measured on a Nikon optical comparator. The average diameter was 29 um with a standard deviation of 5 um. For a first approximation 30 um was used for the diameter of a dot, with a corresponding area of 700 um^2.

Final mathematical calculations with the model to predict the graininess by density function required a value for k. The value for k was obtained by solving equation (21) for k, as shown in equation (27):

$$k = \frac{\bar{D}}{na(1-r_a)} \tag{27}$$

k could best be approximated by producing a high density reflection sample, which would be assigned a particle

reflectance of zero. A reflection sample of 3x magnification with a measured density of 1.82, D = 1.67, $a = 6.3 \times 10^{3}$ um and $n = 1.1 \times 10^{-4}$ was used. The value calculated for k was 2.4. Once the value for k was determined, the particle reflectance for each sample was calculated by solving equation (21) for r_a:

$$r_a = 1 - \frac{\bar{D}}{kna} \qquad (28)$$

The value of D used was the average reflection sample density minus the substrate density measured on the microdensitometer. With these values equations (22) and (23) could be used to calculate WS(0), and finally the graininess value for each reflection sample.

A comparison was then made of the measured graininess values vs. the calculated graininess values to determine the accuracy of the model. The graininess by density matrix of reflection samples was then assembled. Samples of even values of graininess from 2 to 30 were presented. The density range of 0.0 to 1.4 was presented in twelve steps of equal size in Munsell space. Equal differences in Munsell value correspond to equal visual differences in brightness. Figure 9 is an abbreviated example of the graininess by density matrix.

CHAPTER V

RESULTS AND DISCUSSION

The graininess by density function has been mathematically modeled and a graininess by density matrix has been produced. Figure 9 is an abbreviated version of the graininess by density matrix. Figure 10 describes the matrix composition. Figure 11 shows calculated values of graininess for the 1X, 2X, and 3X cases. The graininess values peak at mid-densities because of two limits operating at the low and high densities. At low densities, there are few particles and, hence, little power in the Weiner Spectrum. At high densities there is much greater noise power but the eye is not sensitive to density fluctuations at these levels. Therefore the graininess peaks at mid-densities, in this case around 0.7 absolute density units.

The plots presented in Figure 12 are the graininess values calculated by computer using equation (3). They will be referred to as the "measured" data. The Figures 13 and 14 are computer output for two samples. Both samples were made from the 1X plate but at different densities. The output consists of the average measured density, the calculated graininess value and the plot of

the calculated WS(u). Note the decreasing power of the WS(u) with a decrease in density. The WS(u) is not constant, whereas a constant WS(u) was assumed for the graininess by density model. The general shape of the measured graininess by density functions are predicted by the calculated data. The calculated data falls short of matching the peaks of the measured data and does not fall off as rapidly at the high densities. The plots in Figure 15 of the ratio of measured graininess value to calculated graininess value for a given density show that the measured value is always greater than the calculated value up to a density of 1.20. In the density range of 0.4 to 1.2, the ratio is typically 1.3. The measured values were expected to be greater than the calculated values if the dots overlapped. Refer to reference 14 by B. Bayer. Figure 16 is a photomicrograph of a graininess sample. It is obvious that the dots are not round and are clumping to form aggregates. These conditions would contribute considerably to theoretical error. It is not surprising that this model does not accurately describe the calculated results. However the model was useful in empirical terms to show the feasibility of matrix production and to suggest initial experimental values of magnification and density that would produce a specific graininess.

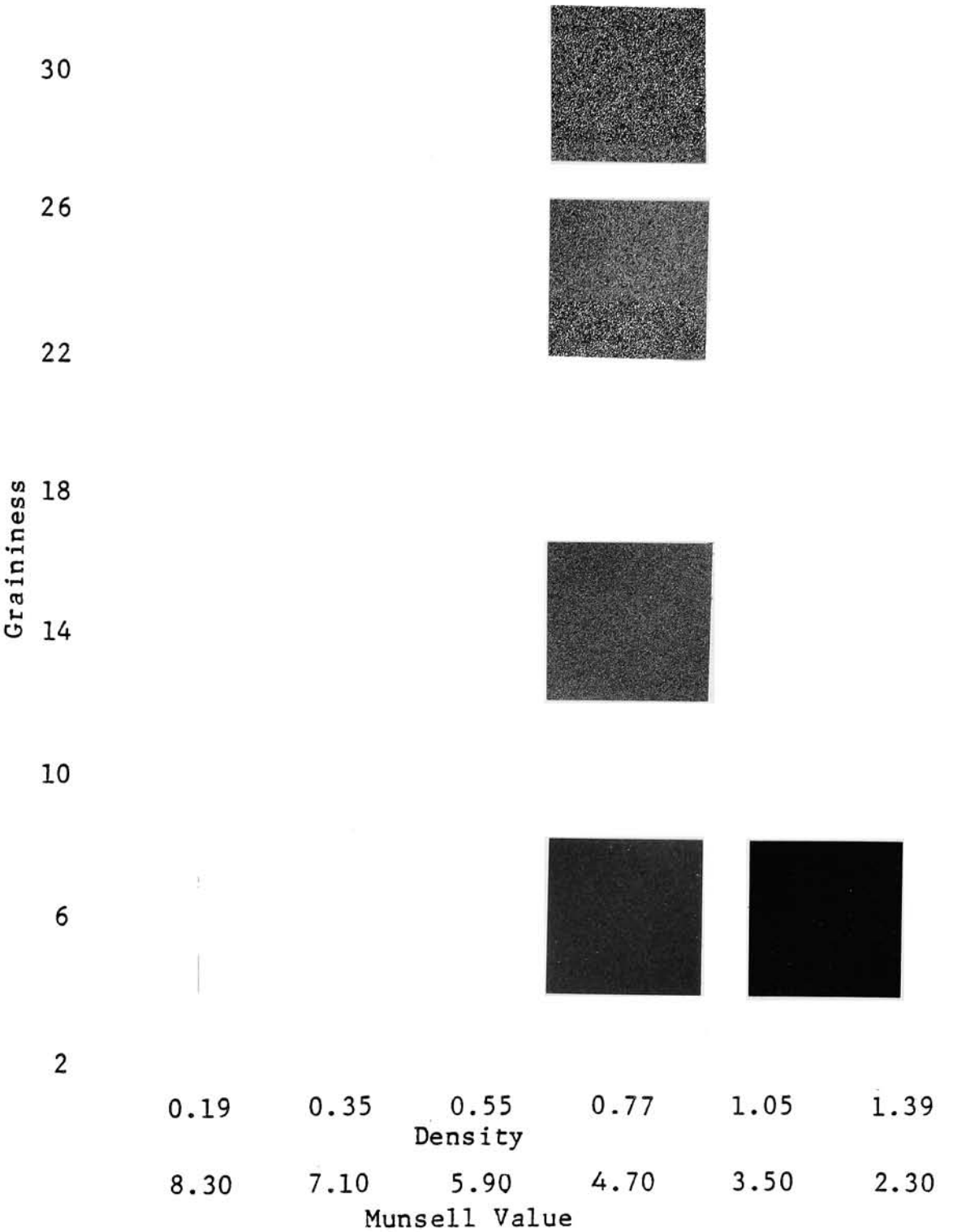

Abbreviated Version of Graininess by Density Matrix

Figure 9

The values presented are: calculated particle reflectance, r_a;
measured Weiner Spectrum value, WS(0);
and sample magnification.

Graininess	0.11	0.19	0.27	0.35	0.45	0.55	0.65	0.77	0.90	1.05	1.21	1.39
30						.74 1005 1.75X	.67 2200 1.75X	.64 2300 1.75X				
28			.92 480 1.5X		.81 870 1.75X		.70 1900 1.75X		.53 4500 1.5X		.41 8000 2X	
26					.81 900 1.75X	.76 1030 1.5X			.55 4200 1.75X		.36 11,800 3X	
24						.76 910 1.5X		.65 1100 1.25X	.58 2800 1.5X			
22									.52 3000 1.25X	.43 3300 1.5X		
20				.87 280 1.75X	.83 500 1.5X					.43 3800 1.25X	.36 5800 1.5X	.28 9000 1.5X
18					.83 250 1.25X							
16		.91 100 1.75X					.72 700 0.8X	.65 1200 0.8X	.54 2100 0.8X	.46 3200 0.8X	.38 4600 1.25X	.25 5300 1.5X
14			.93 82 1.75X	.89 220 1.5X	.82 320 0.8X		.72 350 1X	.63 390 1X	.57 1000 1X			.27 4500 1.75X
12		.99 59 1.5X	.92 120 1.5X	.89 150 0.8X	.85 230 0.8X					.50 1000 1X		.27 4000 1.25X
10		.92 40 1X	.88 100 1X							.44 750 1X		
8		.96 30 0.8X		.89 90 1X	.82 100 1X	.75 150 0.8X	.70 400 0.8X	.65 450 0.8X				
6			.93 32 0.8X	.87 75 0.8X	.82 160 0.8X	.77 130 0.8X		.66 260 0.8X	.55 320 0.8X	.45 700 0.8X	.37 750 0.8X	
4		.99 30 1X	.95 38 0.8X									
2				.86 20 0.8X	.84 24 0.8X							

Density

Munsell Value	8.90	8.30	7.70	7.10	6.50	5.90	5.30	4.70	4.10	3.50	2.90	2.30

Matrix Composition

Figure 10

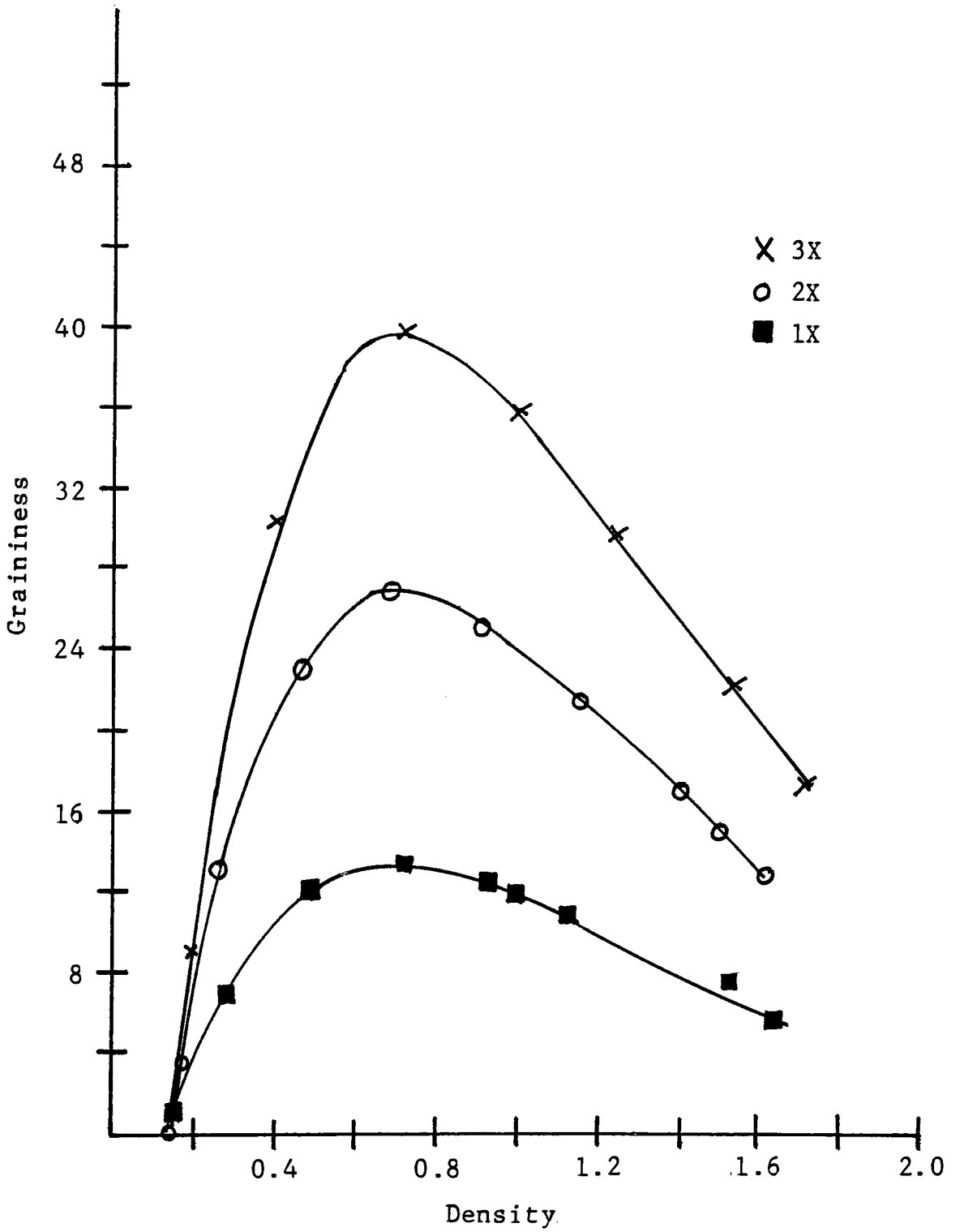

Calculated Graininess Values

Figure 11

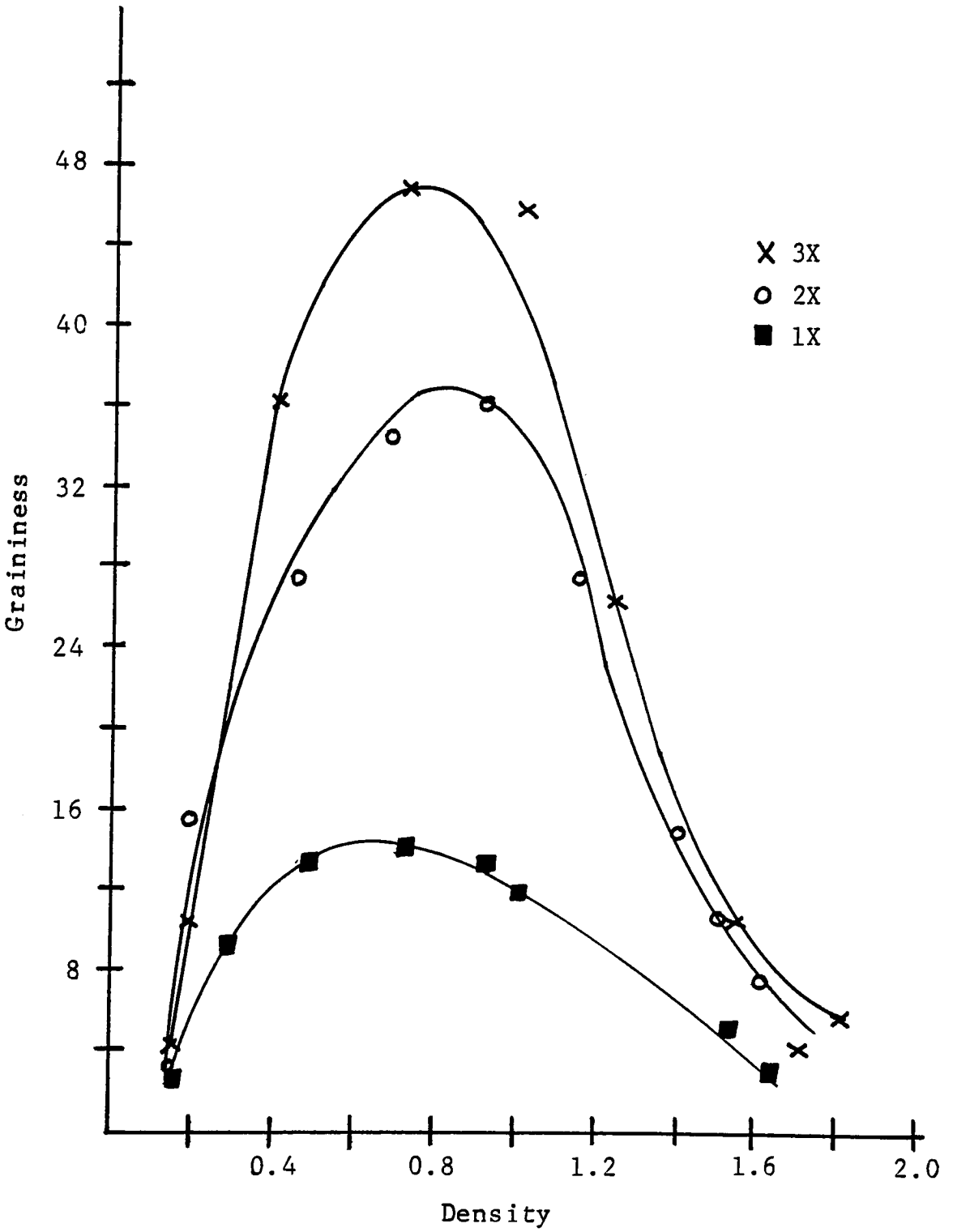

Measured Graininess Values

Figure 12

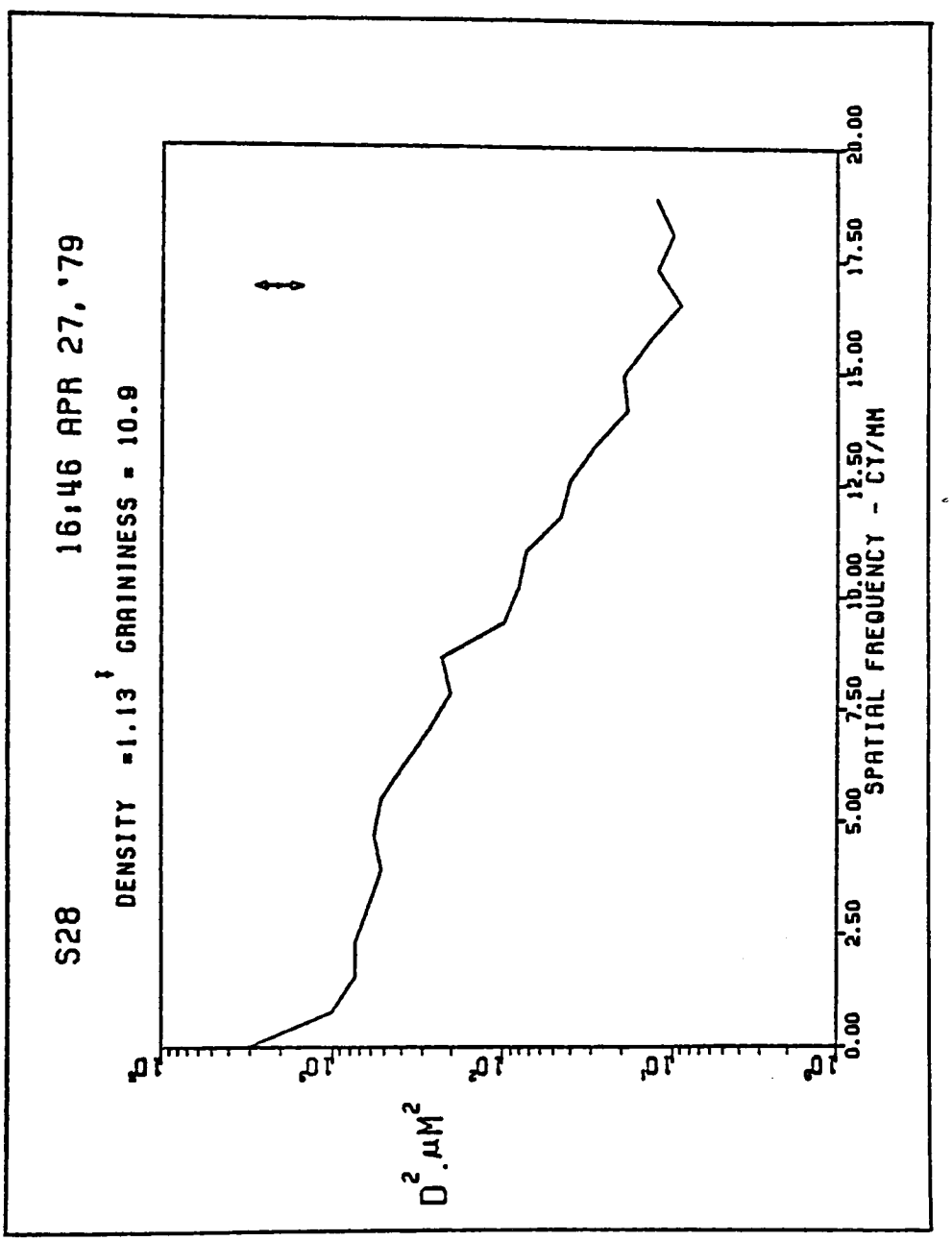

Computer Output for Sample Density = 1.13

Figure 13

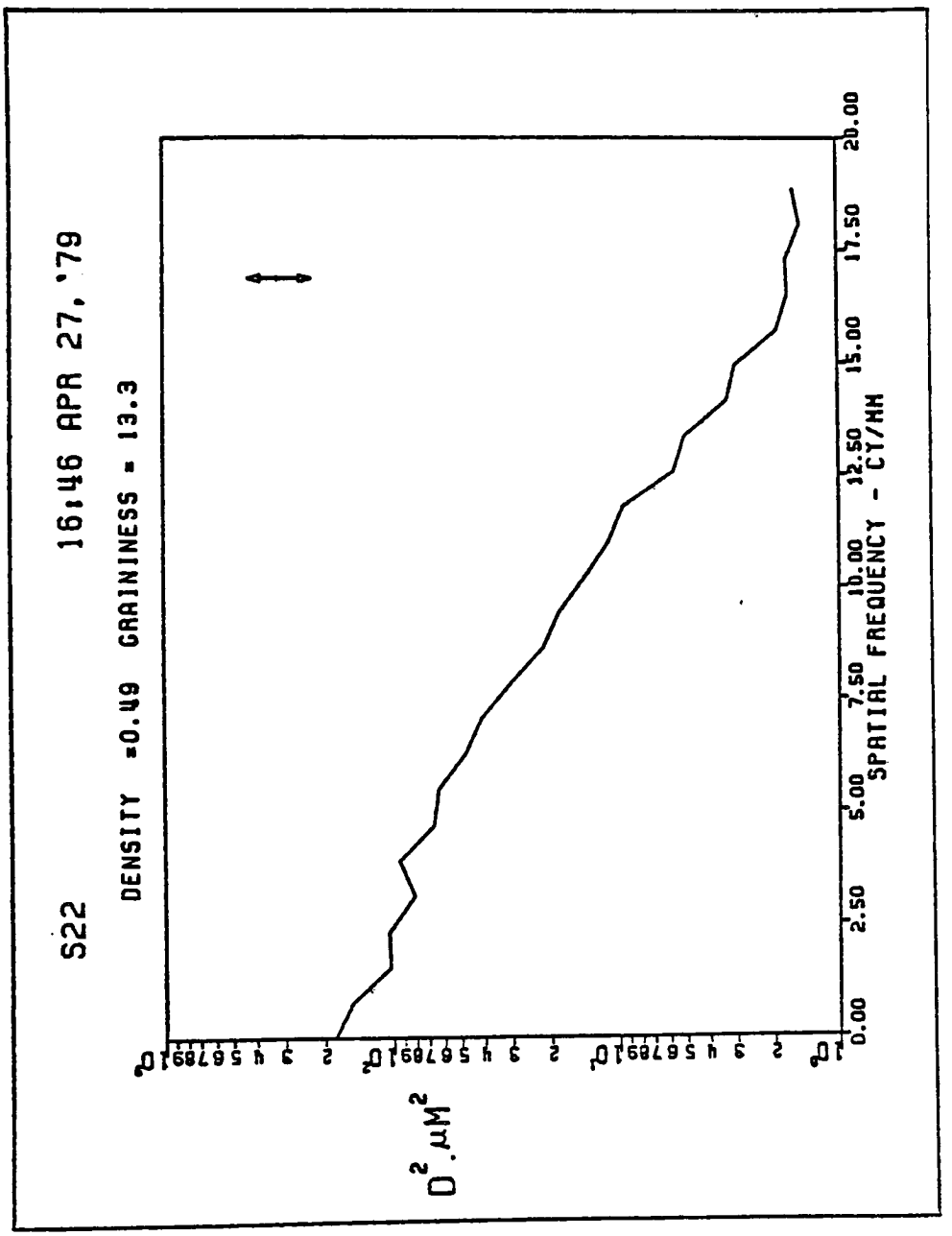

Computer Output for Sample Density = 0.49

Figure 14

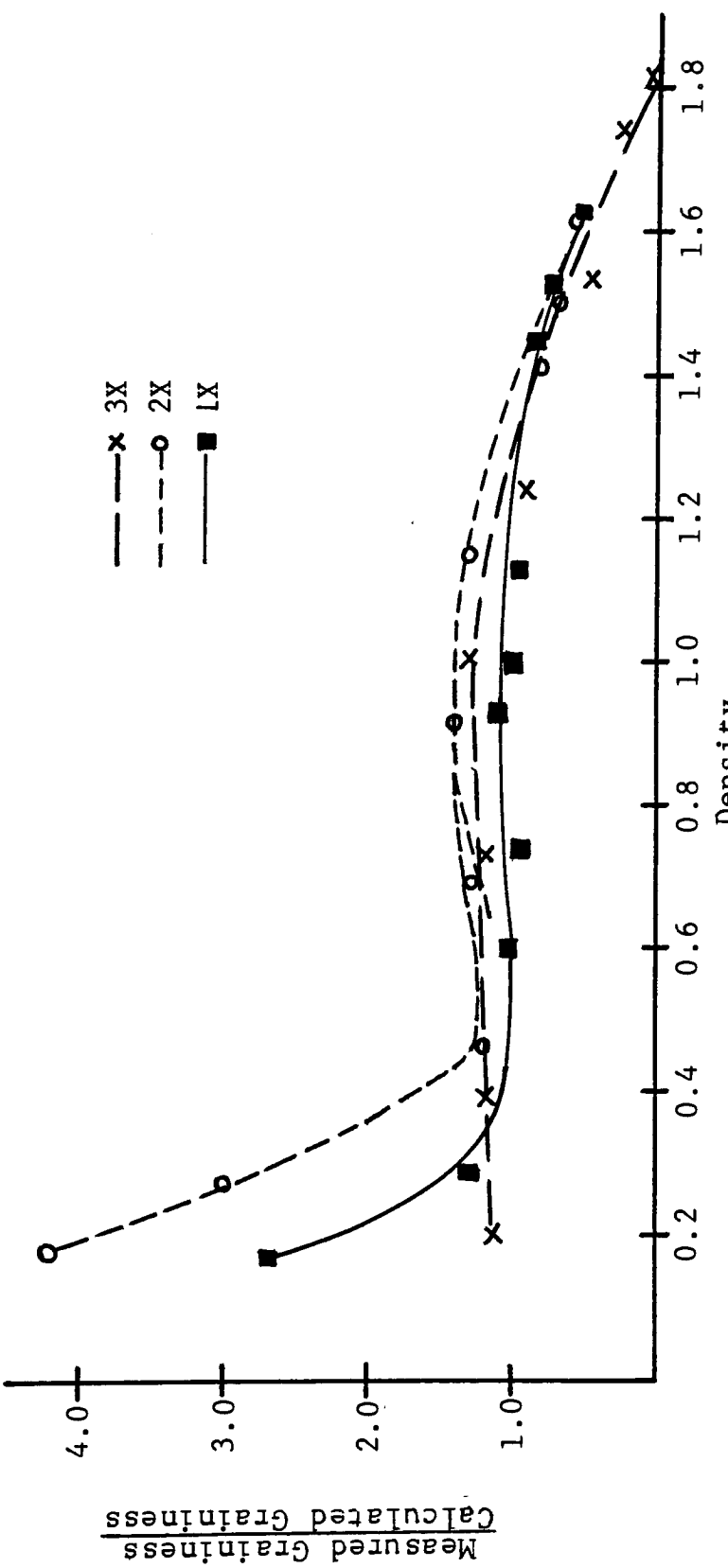

Ratio of Measured to Calculated Graininess Values

Figure 15

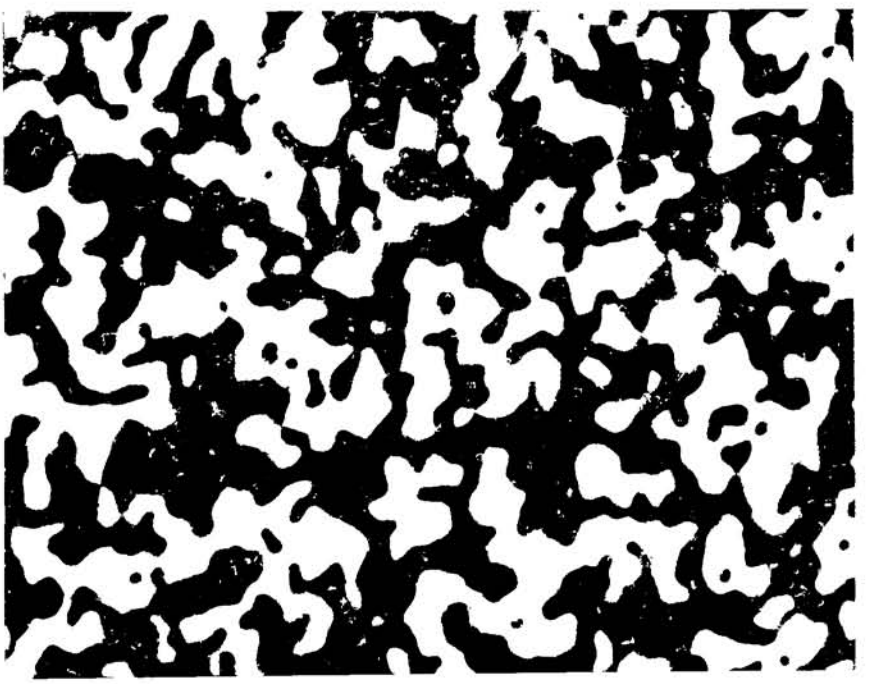

Photomicrograph of 1.75X Sample

Figure 16

APPENDIX A

SIMPLIFIED TUTORIAL ON WEINER SPECTRUM

Noise in an electrical signal may be observed with an oscilloscope trace as voltage fluctuations about a mean level. This is illustrated in Figure A1. This noise may also be characterized by the power at given frequencies of interest. Figure A2 is a plot of power vs. frequency.

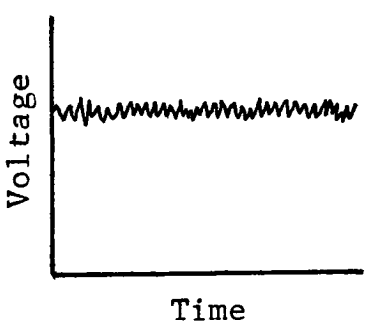

Typical Oscilloscope Trace

Figure A1

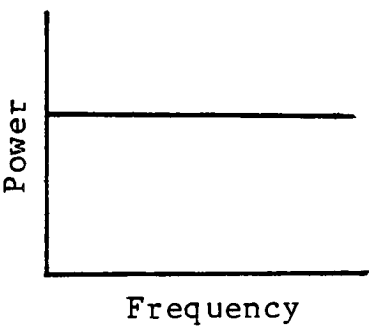

Power Spectrum

Figure A2

This plot is called a power spectrum for "white noise". White noise is equal power at all frequencies of interest. The mathematics that explains how to transform Figure A1's data to Figure A2 is termed Fourier Theory. The power spectrum will change with the electrical signal.

A sinusoidal signal as in Figure A3 will have a power spectrum as in Figure A4.

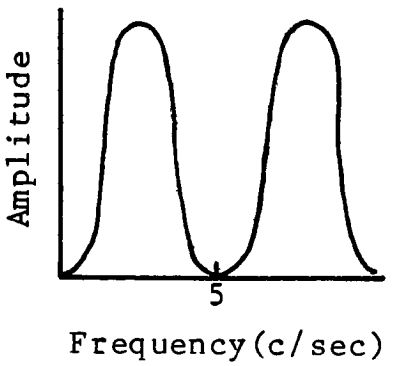

Sinusoidal Signal

Figure A3

Power Spectrum
for Sinusoidal Signal

Figure A4

Only frequencies at 5 c/sec are present in the signal, therefore one would expect to find power at that frequency and no other. Superimposing the signal of Figure A3 over the white noise signal of Figure A1 will result in the power spectrum of Figure A5 on the following page. There will be equal power at all frequencies except for 5 c/sec where there will be a power spike.

The random structure in a two dimensional photographic image is an equivalent noise phenomona to the electrical example, above. The density fluctuations due to the grain may be observed with a microdensitometer scan. Refer to Figure A6 on the next page.

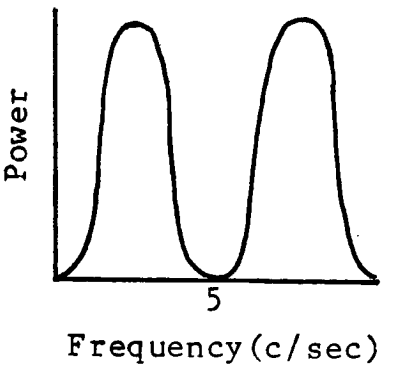

Power Spectrum

Figure A5

D_1 is the mean density level of the sample about which the density fluctuations occur. Figure A6 is random noise fluctuation. Applying the Fourier mathematics, this signal may be transformed, just as an electrical signal is transformed, to show the power at a given frequency range. Image scientists prefer to call the plot of Figure A7 Weiner Spectrum rather than power spectrum, but the

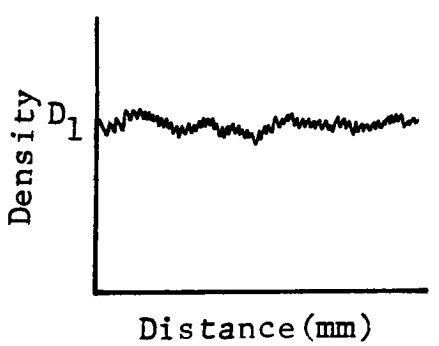

Microdensitometer Scan of Random Grain Distribution

Figure A6

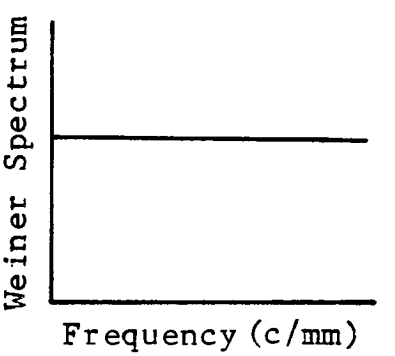

Weiner Spectrum of Random Grain Distribution

Figure A7

parallel concepts between the image science and the electronics still holds. Wiener Spectrum is restricted to "smooth spectrums" i.e. no power spikes as in Figure A5. This does not imply a flat spectrum as in Figure A7. Figure A8 is also a Wiener Spectrum.

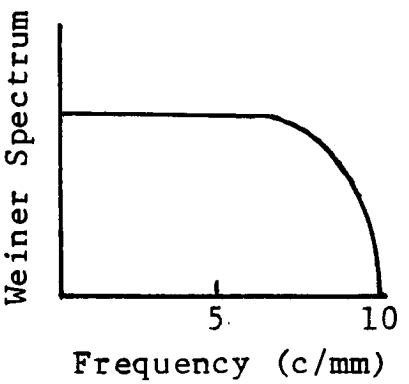

Weiner Spectrum of
Random Grain Distribution
and Limited Grain Size

Figure A8

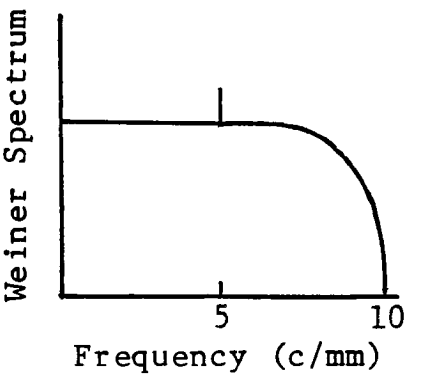

Weiner Spectrum of
Non-Random Sample

Figure A9

The spectrum falls off at a given frequency due to the particle sizes present in the image. There is no information beyond 10 c/mm. It should now be possible to see that a photographic sample of uniform density that has grain particles of random size and positioning within the sample will be analagous to white noise and will have a Weiner Spectrum like Figure A8 that is flat to the frequency cutoff of the particle size. Similarly if a sinusoidal image of 5 c/mm (Figure A3) is imaged onto film it is expected the power spectrum would be similar to Figure A9.

In this application it is desirable to have a smooth WS without any power spikes. This indicates a sample that has grain particles of random positioning.

APPENDIX B

SIMPLIFIED TUTORIAL ON MODULATION TRANSFER FUNCTION AND VISUAL TRANSFER FUNCTION

The Modulation Transfer Function is a measurement used to describe the ability of film and optical components to reproduce the detail in an object. The Visual Transfer Function is a similar measurement used to describe the capability of the human eye. Both functions are strictly applicable only to linear systems, that is, systems which do not change their characteristics as other variables change.

It is possible to characterize an audio amplifier by putting in sinusoidal signals of different frequencies and measuring the ratio of the output amplitude to the input amplitude. This ratio is called gain:

$$\text{Gain} = \frac{\text{Voltage out}}{\text{Voltage in}} \qquad \text{(B1)}$$

Refer to Figure B1, on the next page.

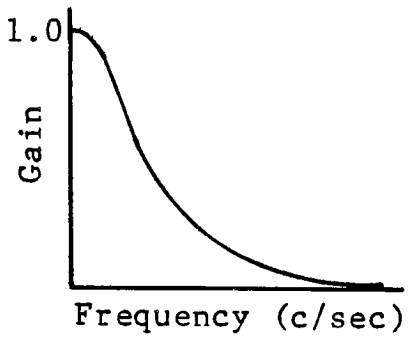

Gain vs Frequency

Figure B1

MTF and VTF are analogous to gain. Instead of inputting a signal that varies with time i.e. cycles/sec., the signal changes with distance in cycles/mm as in Figure B2. These light and dark stripes may be called a sinusoidal grating.

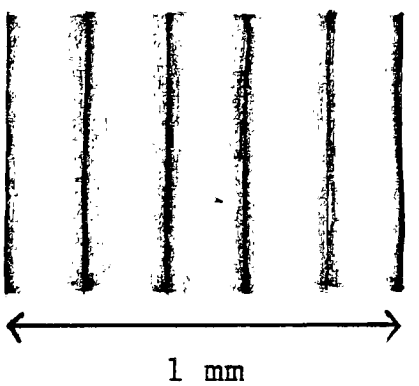

A 5 c/mm Signal

Figure B2

The MTF is measured by inputting a signal sinusoidal in transmittance with a certain contrast or modulation and measuring the modulation of the signal after it passes through the system.

$$MTF = \frac{\text{modulation out}}{\text{modulation in}} \qquad \text{where:} \quad (B2)$$

$$\text{modulation} = \frac{T_{max} - T_{min}}{T_{max} + T_{min}} \qquad (B3)$$

T_{max} and T_{min} are the maximum and minimum transmittances in the grating.

The VTF is measured differently because one is dealing with the human eye and the system output is not directly measurable. This problem is ordinarily overcome by assuming that the detection thresholds for gratings of different frequencies represent equivalent system outputs. With this assumption, the transfer function can be determined by increasing the modulation of each grating until it can just be detected.

To facilitate comparison of MTF and VTF curves, the VTF is defined as the reciprocal of the detection threshold vs. frequency and is normalized to 1.0 at low frequency. This interpretation of the VTF is presented in Figure B3 for the range of frequencies over which the graininess integral is calculated. The data for this

curve comes from several measurements in the general literature[1], and the abscissa is scaled for a viewing distance of 35 cm. At this distance the curve is effectively zero at 8 c/mm, meaning that this is the highest spatial frequency which humans can detect.

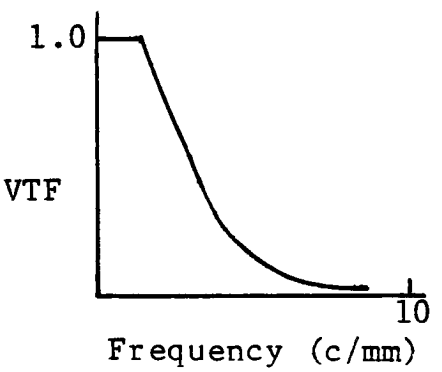

Visual Transfer Function

Figure B3

FOOTNOTES FOR APPENDIX B

1. T.N. Cornsweet, Visual Perception, Academic Press, 1971.

APPENDIX C

COMPUTER PROGRAM

Computer Program courtesy of Xerox Corporation.

PROGRAM NAME -----RNDGN-----

```
C      PROGRAM TO UTILIZE RTCC'S GPF TO PRODUCE RANDOM DOT
C      PATTERNS .
       REAL  BUF(128)
C      N     NUMBER OF POINTS WRITTEN
       INPUT N
C       NRET   THE WIDTH OF THE RETICLE IN PIXELS
       INPUT NRET
C       M1     THE MULTIPLIER FOR THE FIRST RANDOM NUMBER
C              GENERATOR
       INPUT M1
C       M2     MULTIPLIER FOR THE SECOND GENERATOR
       INPUT M2
C       S1     SEED FOR THE FIRST RANDOM NUMBER GENERATOR
       INPUT S1
C       S2     SEED FOR THE SECOND RANDOM NUMBER GENERATOR
       INPUT S2
C       IBR    THE BRIGHTNESS OF THE SPOT(0 - 63)
       INPUT IBR
C
C
C      FILL THE INITIAL BUFFER
C
C
       IX=S1
       DO 10  J=1,128
3      IX=IX*M1
       IF(IX) 4,6,6
4      IX=IX+2147483647+1
6      BUF(J)=(IX*1.902452E-06)
       IF (BUF(J).GT.4000.)GO TO 3
10     IF (BUF(J).LT.0)GO TO 3
       CALL GPFPACK('ON')
C
C      THE GPF SPECIFICATIONS ARE SET
C
       CALL PAGEROTN('LP')
       CALL PEXTENT(1.,1.,5000.,4000.)
       CALL BRIGHT(IBR)
C
```

```
C      THE POINT ADDRESSES ARE CHOSEN FROM THE INITIAL
C      BUFFER
       IXX=S2
       DO 20 J=1,N
2      IXX=IXX*M2
       IF (IXX)7,8,8
7      IXX=IXX+2147483647+1
8      JY=IXX*.6087846E-07
       IF (JY.GT.128) GO TO 2
       IF (JY.LT.1) GO TO 2
       POSY=BUF(JY)
C
C
C      THE Y POSITION IN THE INITIAL BUFFER IS REFILLED
C
C
16     IX=IX*M1
       IF(IX) 12,13,13
12     IX=IX+2147483647+1
13     BUF(JY)=IX*1.9024520E-06
       IF(BUF(JY).GT.4000.)GO TO 16
       IF(BUF(JY).LT.0.) GO TO 16
C
C
C      THE X POSITION IN THE INITIAL BUFFER IS CHOSEN
C
C
1      IXX=IXX*M2
       IF(IXX)9,11,11
9      IXX=IXX+2147483647+1
11     JX=IXX*.6087846E-07
       IF (JX.GT.128) GO TO 1
       IF (JX.LT.1) GO TO 1
       IF (JX.EQ.JY) GO TO 1
       POSX=BUF(JX)
C
C
C      THE X POSITION IN THE INITIAL BUFFER IS REFILLED
C
C
17     IX=IX*M1
       IF(IX)14,15,15
14     IX=IX+2147483647+1
15     BUF(JX)=(IX*1.9024520E-06)
       IF(BUF(JX).GT.4000.) GO TO 17
       IF(BUF(JX).LT.0.) GO TO 17
C
```

```
C     THE GPF IS CALLED
C
C
      CALL MOVE(POSX,POSY)
      CALL POINT
C
      A=A+1
20    CONTINUE
C
C
C     A RETICLE IS DRAWN ON THE EDGE OF THE SAMPLE
C
C
      DO 30 J=1,NRET
      ZI=FLOAT(4200+J)
      CALL MOVE(ZI,0000.)
      CALL DRAW(ZI,4000.)
      ZI=FLOAT(1998+J)
      CALL MOVE(4100.,ZI)
      CALL DRAW(5000.,ZI)
30    CONTINUE
      CALL GPFPACK('OFF')
      WRITE(106,90)   A
90    FORMAT(3X,'NUMBER OF POINTS WRITTEN=',E14.6)
      WRITE(106,91) S1,M1
91    FORMAT(3X,'POSITION GENERATOR SEED=',I10,'MULTIPLIE='
      I10)
      WRITE(106,92) S2,M2
92    FORMAT(3X,'ARRAY POSITION GENERATOR SEED=',I10,
      'MULTIPLIER=',I10)
      STOP
      END
```

APPENDIX D

PROCESSING FOR RECORDAK AHU MICROFILM

Chemistry at 72° F., Processed in Nikor tank.

Solution	Dilution	Time (min.)
Eastman Kodak Prostar developer	-	6.0
Stop	-	0.25
Rapid fix	-	2.0
Running water rinse	-	10.0
Photo-flo	-	1.0
Dry		

PROCESSING FOR CHRONAPAQUE PAPER

OC safelights

Solution	Dilution	Time (min.)
Dektol	1:2	1.5
Stop Bath	-	0.25
Fix	-	2.0
Wash	-	8.0

REFERENCES

1. Shaw, R. (Ed.), Selected Readings in Image Evaluation, (SPSE Publication,1976).

2. Marriage, A. and Pitts, E.,"Relation between Granularity and Auto-correlation",J. Opt. Soc. of Amer., 46, 1019-1027.

3. Shaw, R.,"Equivalent Quantum Efficiency of Photographic Emulsions", J. Phot. Sci., 13, 1965, 308-317.

4. Ericson, R.H. and Marchant, J.C., "RMS Granularity of Monodisperse Photographic Emulsions", Phot. Sci. Eng., 16, 1972, 253-257.

5. Shaw, R., "Comparative Signal-to-Noise Ratio Analysis of Particle Development in Electrophotography and Silver Halide Photography", J. Appl. Phot. Eng., 1, 1975, 1-4.

6. VanEngeland, J., Verlinden, W., and Marien, J., "Granularity of Electrophotographic Images", J. Phot. Sci., 25, 1977, 154-158.

7. Goren, R.N. and Szczepanik, J.F., "Image Noise of Magnetic Brush Development", Photo. Sci. Eng., 22, 1978, 235-239.

8. Dainty, J.C. and Shaw, R., Image Science (Academic Press, 1974), 58-60, 98.

9. Dooley, R.P., and Shaw, R., "Noise Perception in Electrophotography", J. Appl. Phot. Eng., 4, 1979, 190-196.

10. Dainty, J.C., Laser Speckle, Springer, 1976.

11. Yasuda, Yoshizumi, "Subjective Evaluation on the Noise on Image", Proceedings SPSE Tech. Conf. 10/24-25, 1977.

12. Scott, F.S., "Photographic Image Simulation", J. Photo. Sci., 12, 139-142.

13. Personal correspondence with James J. Jakubowski, Xerox employee, Webster, N.Y.

14. Bayer, B. E., "Relation Between Granularity and Densityfor a Random-Dot Model", J. Opt. Soc. of Amer., 54, 1964, 1485-1490.

15. Berwart, L., "Weiner Spectrum of Experimental Emulsions with Cubic Homogeneous Grains, Comparison of the Spectra with the Wiener Spectra of Commercial Emulsions", J. Phot. Sci., 17, 1969, 41-47.

16. Cornsweet, T.N., Visual Perception, Academic Press, 1971.